Biochemical Pharmacology 83 (2012) 78–87

Contents lists available at SciVerse ScienceDirect

Biochemical Pharmacology

journal homepage: www.elsevier.com/locate/biochempharm

Sam68 interacts with IRS1

R. Quintana-Portillo [a], A. Canfrán-Duque [a], T. Issad [b,c,d], V. Sánchez-Margalet [a], C. González-Yanes [a,*]

[a] Department of Clinical Biochemistry, Virgen Macarena University Hospital, University of Seville, Av. Dr. Fedriani 3, Seville 41071, Spain
[b] INSERM U1016, F-75014 Paris, France
[c] CNRS-UMR8104, F-75014 Paris, France
[d] Université Paris Descartes, F-75014 Paris, France

ARTICLE INFO

Article history:
Received 5 August 2011
Accepted 28 September 2011
Available online 10 October 2011

Keywords:
Sam68
IRS1
Insulin receptor
BRET

ABSTRACT

Sam68 (Src associated in mitosis) is a RNA binding protein that links cellular signaling to RNA processing. In previous studies we found that insulin promotes Sam68 relocalization in the cytoplasm allowing Sam68 to associate with p85PI3K, Grb2, GAP and probably the insulin receptor (IR), modulating insulin action positively. In the present work, we wanted to define the role of Sam68 in the first stages of IR signaling.

Both BRET and co-immunoprecipitation assays have been used for the study of Sam68 binding to IR, IRS1 and p85-PI3K.

BRET saturation experiments indicated, for the first time, that Sam68 associates with IRS1 in basal condition. To map the region of Sam68 implicated in the interaction with IRS1, different Sam68 mutants deleted in the proline-rich domains were used. The deletion of P0, P1 and P2 proline rich domains in N-terminus as well as P4 and P5 in C-terminus of Sam68 increased $BRET_{50}$, thus indicating that the affinity of Sam68 for IRS1 is lower when these domains are missing. Moreover, in IR-transfected HEK-293 cells, BRET saturation experiment indicated that insulin increases the affinity between Sam68-Rluc and IRS1-YFP.

In conclusion, our data indicate that Sam68 interacts with IRS-1 in basal conditions, and insulin increases the affinity between these two partners.

© 2011 Elsevier Inc. All rights reserved.

1. Introduction

Sam68 is the Src-associated in mitosis protein of 68 kDa, that belongs to the STAR signal transducer and activator of RNA family of RNA-binding proteins, which are implicated in signal transduction and RNA metabolism [1–3]. Sam68 (Fig. 1) contains a KH domain located within a larger domain of 200 amino acids, with RNA binding activity, named GSG, common to STAR proteins. This GSG domain is flanked by six proline rich sequences (from P0 to P5), located at its N-terminus (P0–P2) and C-terminus (P3–P5) and involved in Sam68 interaction with SH3 and WW domains containing proteins such as Src, Fyn, Sik, BRK [4,5], PI3K [6], PLC-γ-1 [7,8], PRMT [4], Grb2, Grap [9] and Nck [10]. The interaction of Sam68 with the SH3 domains of Src family kinases is required for its tyrosine phosphorylation [2,3]. In fact, Sam68 also contains a tyrosine rich region at the C-terminus of the protein. Tyrosine phosphorylation of Sam68 strongly affects its activity [11] and is necessary for its association with different proteins containing SH2 domains, that include kinases belonging to Src family [2,3,8,12], Sik/BRK [13], as well as those from Itk/Tec family [14,15]. Tyrosine-phosphorylated Sam68 also interacts with docking proteins and signaling enzymes containing SH2 domains such as Grb2 [8,9], Grap [9], Nck [10], PLC-γ-1 [8], Ras-GAP [8,16] and the p85 subunit of PI3K [6]. These numerous interactions suggest that Sam68 plays an adaptor role in signal transduction and is involved in several cellular processes.

We have previously shown the implication of Sam68 in IR signaling. Although Sam68 has been described as a nuclear protein [17,18], it can translocate from nucleus to cytoplasm in presence of methylase inhibitors, viral infections or during cell cycle transition [19–21]. Interestingly, we have demonstrated that Sam68 is exclusively located in the cytoplasm of rat adipocytes and its expression is enhanced upon insulin stimulation. In CHO cells, IR overexpression in itself also increases Sam68 expression, and insulin stimulation further increases its expression and targets Sam68 to the cytoplasm. Moreover, the IR activation *in vivo*, in both CHO-IR cells and rat adipocytes, stimulates Sam68 tyrosine phosphorylation, increasing its association with p85-PI3K [22,23]. In hepatoma cells that over-express IR (HTC-IR), Sam68 is associated with the SH2 domains of the p85 regulatory subunit of PI3K, forming a ternary complex with IRS-1 [24,25]. Furthermore, insulin stimulation promotes Sam68 association with the

* Corresponding author. Tel.: +34 954559852; fax: +34 954907048.
E-mail address: cgyanes@us.es (C. González-Yanes).

0006-2952/$ – see front matter © 2011 Elsevier Inc. All rights reserved.
doi:10.1016/j.bcp.2011.09.030

SH2 domains of GAP *in vivo* and *in vitro* [26,27]. These interactions with insulin signaling effectors suggest that Sam68 plays an adaptor role in IR signal transduction.

Insulin receptor substrates-1 (IRS-1) belong to a family of intracellular proteins with at least six members identified to date (IRS-1 to IRS-6) [28–32]. At first, this family was identified as insulin receptor substrates but now they are also known to be implicated in other signaling pathways. IRS-1 as well as other members of the family contain a Pleckstrin Homology (PH) domain at their N-terminus, that is used to keep the protein bound to membrane phosphoinositides in close proximity to the insulin receptor, and a Phospho-Tyrosine Binding (PTB) domain that recognizes and bind the phosphorylated NPXY motif in the IR [33,34]. IRS-1 also contains numerous tyrosine residues that, once phosphorylated, are recognized by proteins containing Src-homology 2 (SH2) domains such as the p85 regulatory subunit of phosphatidylinositol 3-kinase (PI3K), Grb2, Nck, Crk, Fyn, and SHP-2 [35–37]. Upon insulin receptor activation, IRS-1 is phosphorylated on tyrosine residues, allowing downstream effectors such as PI3K to be recruited and activated. In addition to this canonical role of IRSs in IR and IGFR signaling pathways, IRS-1 and IRS-2 can also interact with many other signaling pathways in a non-canonical way [38] or translocate to the nucleus in response to IGF-I or certain oncogenes (although it does not bear a nuclear localization signal). IRS1 translocation into the nucleus is dependent on its PTB domain. Inside the nucleus, IRS-1 regulates transcription of several genes implicated in different stages of cancer progression. For instance, in the nucleus, IRS-1 associates to estrogen receptor α (ERα) and regulates the ERα gene transcription, inside the nucleus [39,40]. Nuclear IRS-1 also interacts with β-catenin, and regulates the cyclin D1 transcription [38,41].

In this work, our aim was to characterize the role of Sam68 in IR signaling pathway by BRET. The BRET technology is an important tool for the study of protein–protein interactions in living cells [42,43]. The use of this methodology has allowed us to describe, for the first time, the direct interaction between Sam68 and IRS1 as well as the regions of Sam68 involved and the implication of the said interaction in IR signaling.

2. Materials and methods

2.1. Reagents and materials

2-Amino-2-(hydroymethyl)-1,3-propanediol (Trizma base), sodium orthovanadate, pyrophosphate tetrasodium salt, sodium fluoride, Tween-20, Triton X-100, poly-L-lysine-hydrobromide and paraformaldehyde were from Sigma (St. Louis, MO, USA). phosphate buffer saline (PBS) was from BioWhittaker (Lonza, VerviersBelgium). Nonidet-P40 was from Fluka-Biochemika

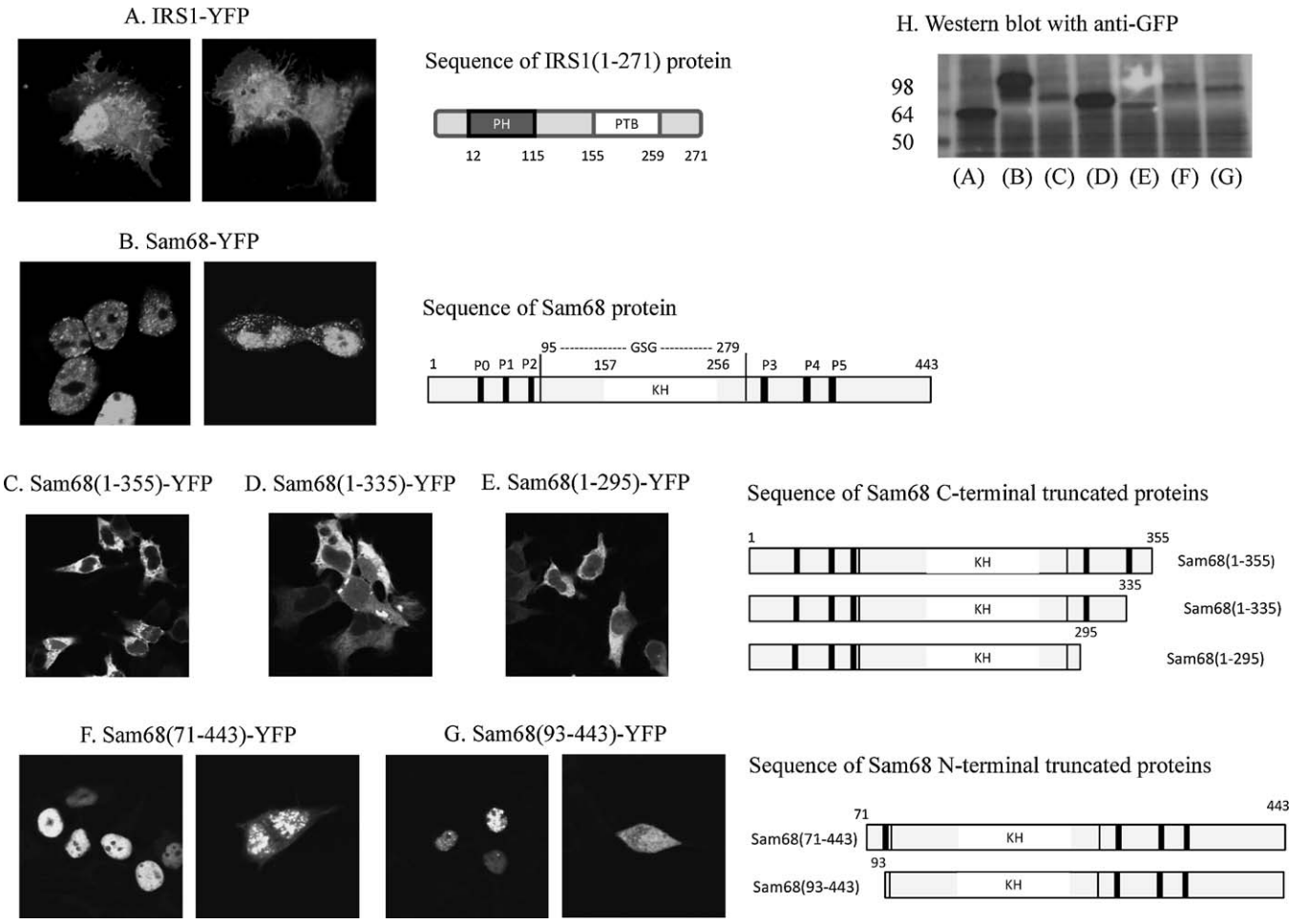

Fig. 1. Expression of yellow fluorescent protein (YFP) fusion constructions in human embryonic kidney (HEK)-293 cells. Cells were transfected with cDNAs encoding YFP-tagged proteins. The confocal images show the localization of each protein expressed. A schematic diagram of each protein is shown alongside the fluorescence image: (A) expression of IRS1(1–271)-YFP, (B) wild-type Sam68-YFP (C), Sam68(1–355)-YFP, (D) Sam68(1–335)-YFP and (E) Sam68(1–295)-YFP, (F) Sam68(71–443)-YFP and (G) Sam68(93–443)-YFP. The percentage of transfected cells showing a high fluorescence signal was around 25–30%. (H) Western blot showing the expression level of each construction. HEK293 cells were transfected with 600 ng of cDNAs, lanes (A) IRS1-YFP, (B) Sam68-YFP, (C) Sam68(1–335)-YFP, (D) Sam68(1–355)-YFP, (E) Sam68(1–295), (F) Sam68(71–443) and (G) Sam68(93–443). Two days after transfection, cells were lysed and immunoblotted with anti-GFP antibody.

(Sigma Aldrich, St. Louis, MO, USA and Steinheim, Germany). Other chemicals were from Panreac (Barcelona, Spain).

Insulin actrapid© was purchased from Novo Nordisk (Bagsvaerd, Denmark). Protein G-sepharose, nitrocellulose membranes, and Hyperfilm ECL were from GE healthcare (Upsala, Sweden and Buckinghamshire, UK). Western-Blotting luminol reagent was from Santa Cruz Biotechnology (Santa Cruz, CA, USA). Glycerol, protease inhibitor cocktail and Fugene 6 transfection reagent were from Roche (Mannheim, Germany).

Recombinant YFP protein was from BioVision (San Francisco, CA, USA). Coelenterazine h was purchased from Uptima, Interchim (Montluçon, France). Phusion hot Start high fidelity DNA polymerase was from Finnzymes (Espoo, Finland). ApaI, KpnI and EcoRI restriction enzymes were from Takara Bio Inc. (Shiga, Japan).

2.2. Antibodies

Monoclonal anti-GFP antibodies were purchased from Roche (Mannheim, Germany); antibodies against insulin receptor β-subunit (C-19): sc-711 and Sam68 (C-20): sc-333, were purchased from Santa Cruz Biotechnology. Monoclonal antibody to Renilla Luciferase was from Chemicon International (Temecula, CA). Sheep anti-mouse and donkey anti-rabbit, IgG HRP-linked whole antibodies were from GE healthcare. Anti-mouse-IgG-Atto 633 from goat antiserum was from Fluka (Sigma Aldrich, Steinheim, Germany).

2.3. Expression vectors

The complementary DNA encoding IR–Rluc, IRS(1–271)-1-YFP, and IR-pcDNA3.1 have been described previously [44–46]. p85α-YFP was kindly provided by Dr. G. Bismuth. Wild-type Sam68 sequence was subcloned in frame with the YFP coding-sequence in the pEYFP-N1 expression vector (Clontech:Takara Bio Inc., Shiga, Japan), using sites in the polylinker of the vector. To clone Sam68 in phRLuc-N3 expression vectors the sites chosen were KpnI and ApaI. For truncated forms of Sam68, the same sites were used to clone them in eYFP-N1 and phRLuc-N3 vectors. In Sam68(71–443) protein the 70 first amino acids of Sam68 containing proline rich domains P0 and P1 are missing. In Sam68(93–443) the first N-terminal 92 aminoacids containing P0, P1 and P2 rich proline domains are missing. The C-terminal deleted mutants of Sam68 are Sam68(1–355) lacking 88 aminoacids comprising P5 proline rich domain, Sam68(1–335) lacking P5 and P4 proline rich domains and Sam68(1–295) lacking P5, P4 and P3. The cDNA sequences of these proteins were cloned by PCR excluding the above mentioned segments and introduced between EcoRI and ApaI sites in EYFP-N1 and between KpnI and ApaI in phRLuc-N3 expression vectors.

2.4. Cell culture and transfection

HEK-293 cells were seeded at a density of 2×10^5 cells per 35-mm dish, and were transfected one day later with cDNA coding for IR-Luc and Sam68-YFP or Sam68-Luc and IRS1-YFP as specified in the figure legends. One day after transfection, cells were transferred into polylysine-coated 96-well microplates (CulturPlate-96, white; NUNC, Thermo Scientific, Roskilde, Denmark) at a density of 3×10^4 cells per well. BRET measurements were carried out in these microplates on the following day [44,47].

2.5. BRET measurements

All BRET measurements were performed at 21 °C using a TriStar LB941 microplate analyser (Berthold, Bad Widbad, Germany). Cells grown in 96-well microplates were washed once with PBS and pre-incubated for 15 min in PBS in the presence of 5 μM coelenterazine h (the luciferase substrate). Light-emission acquisition at 485 and 530 nm was then started and prolonged for 20 min. In some cases, insulin (100 nM) was added after 15 min of pre-incubation with coelenterazine and acquisition was started immediately. Cells expressing only the protein fused to RLuc (BRET donor) were used to determine the background. BRET measurements were carried out every 24 s and repeated 30 times. BRET signal was expressed in milliBRET units (mBU) as previously described [44].

For BRET saturation experiments, constant amounts of the cDNA coding for the Luc-tagged partner were co-transfected with increasing amounts of cDNA coding for the YFP-tagged partner. 48 h after transfection, BRET measurements were performed as described previously. The data were plotted as a function of the YFP/Luc ratio and analyzed with a nonlinear hyperbolic regression using the GraphPrism 5 software (GraphPad Software, San Diego, CA, USA). To determine [YFP]/[Luc] ratio, luciferase expression level was determined by measuring the total luciferase activity in the cells, and YFP expression level was determined by measuring the fluorescence signal emitted by the cells at 530 nm after illumination at 480 nm. These signals were converted into moles of YFP and luciferase using regression curves. The regression curve for YFP was obtained by measuring the fluorescent signal emitted by a recombinant commercial protein purchased from Biovision. Dilutions of a 2 mg/ml-stock solution of YFP were prepared in PBS and the fluorescent signal emitted by 30, 60, 100, 150, 300, 500, 700, 1000 and 1500 ng was measured. Plotting the fluorescent signal as a function of ng of YFP recombinant protein (converted to nmoles) gives the equation that permit to convert fluorescent signal into nmoles of protein. For luciferase regression curve, HEK293 cells were transfected with crescent amounts of a cDNA encoding luciferase fused to YFP (a Luc-YFP fusion protein). The luciferase activity and fluorescence level in these cells were then measured. Using the regression curves obtained with recombinant YFP, the expression of YFP could be converted in nmoles, and therefore the luciferase activity could be also expressed in nmoles (one molecule of Luc is associated with one molecule of YFP in the fusion protein). A regression curve to convert luciferase activity into nmoles was therefore obtained by plotting the luminescent signal as function of nmoles of YFP protein. The software used to fit the regression data was GraphPrism 5.

2.6. Fluorescence imaging

HEK293 were plated at a density of 2×10^5 cells per 35-mm dish on poly-L-lysine (1.5 μg/ml)-pre-coated glass coverslips. The day after cells were transfected with 300 ng of Sam68-YFP, Sam68(1–355)-YFP, Sam68(1–335)-YFP, Sam68(1–295)-YFP, Sam68(71–443)-YFP or Sam68(93–443)-YFP cDNAs. 48 h after transfection, cells were washed 3 times with PBS and fixed with paraformaldehyde (4%) in PBS for 20 min and washed again 3 times in PBS. The coverslips were then mounted over a microscope slide with one drop of mounting medium (Fluoromount, SouthernBiotech, Birmingham, AL, USA). Immunofluorescence images were collected in a laser scanning spectral confocal microscope (Laser Leica TCS-SP2, Wetzlar, Germany).

2.7. Immunocytochemistry in HEK293 cells

The subcellular localization of Sam68-Luc/IRS1-YFP interaction was studied by confocal microscopy. HEK293 cells were co-transfected with both constructions and 24 h later plated on poly-L-lysine-coated coverslips, and then and allowed to attach overnight. The next day, in a dark place, cells were fixed for 20 min in a 4% paraformaldehyde solution, subsequently rinsed 3 times in PBS pH 7.4 and blocked for 1 h in PBS containing 2% bovine serum

albumin (BSA) and 0.1% (v/v) Triton X-100 for permeabilization. Next, cells were incubated for 4 h a room temperature with an anti-luciferase antibody dilution (1:100 in PBS containing 2% BSA and 0.025% (v/v) Triton X-100). Then, coverslips were rinsed 3 times with PBS and incubated for 1 h at room temperature with a 1:500 (v/v) dilution of an atto 633-conjugated goat anti-mouse antibody in PBS containing 2% BSA and 0.025% (v/v) Triton X-100. After extensive washing with PBS, the coverslips were drained and mounted onto glass slides using a drop of mounting medium. A control for primary antibody was made in cells non transfected with Sam68-Luc. A control for secondary antibody also was made in absence of primary antibody, in cells co-expressing both constructions.

2.8. Western blotting

In order to evaluate the level of protein expression in HEK-293 cells transfected for BRET experiments, a fraction of the transfected cells were not transferred in 96 well microplates but spared for seeding in a 6-well plate. 24 h after, these cells were lysed with extraction buffer (i.e., at the same time as BRET measurements). Total lysates were subsequently incubated 20 min at 4 °C and insoluble proteins pelleted-off by centrifugation. The soluble supernatants were denatured with loading buffer [48] for 5 min at 95 °C, resolved by SDS-PAGE and electrophoretically transferred onto nitrocellulose membranes. The membranes were blocked 1 h at room temperature in PBS-T (PBS with 0.2% of Tween 20) containing 3% of BSA. The blots were then incubated with primary antibodies for 3 h at RT or overnight at 4 °C, washed 3 times in PBS-T, and further incubated with a secondary antibody linked to horseradish peroxidase. Bound horseradish peroxidase was visualized in hyperfilm ECL by using a western blotting luminol reagent from Santa Cruz.

2.9. Co-immunoprecipitation of Sam68 and IRS1

HEK-293 cells grown in 10-cm dishes were transiently transfected with the cDNA coding for IRS-YFP and Sam68 wild-type or Sam68 deletion mutants fused to luciferase. 48 h after transfection, the cells were washed in cold PBS and lysed for 30 min at 4 °C with 1 ml of ice-cold lysis buffer (50 mM Tris pH 8, 1% Nonidet P-40, 137 mM NaCl, 10% glycerol, 1 mM phenylmethylsulfonyl fluoride, 1 mM sodium orthovanadate, 50 mM NaF, 10 mM pyrophosphate and protease inhibitor cocktail). Protein concentration was determined by the BCA protein assay kit from Pierce using BSA as standard. Soluble cellular lysates were incubated with anti-GFP antibody for 3 h at 4 °C. Next, 50 μl protein G-Sepharose was added to immune complexes, and incubation was continued for 2 h at 4 °C [49]. The immunoprecipitates were washed 3 times with lysis buffer and proteins denatured with 40 μl of loading buffer [48] for 5 min at 95 °C. The soluble supernatants were then resolved by SDS-PAGE and electrophoretically transferred onto nitrocellulose membranes perform western blotting.

3. Results

3.1. Study of wild-type and Sam68-YFP deleted mutants' localization

As shown in Fig. 1, the localization of the fusion proteins is consistent with that previously described by others [17,18,50,51]. Fig. 1A shows that IRS1(1–271)-YFP is essentially located in the cytosol, but some cells also display a dual cytosolic and nuclear localization. The isoform of IRS1 used comprises the first 271 in N-terminus containing the PH and PTB domains of IRS1, because full length IRS1-fluorescent protein fusion is not properly expressed and forms aggregates in the cell ([51] and our unpublished observations). Cells expressing Sam68-YFP (Fig. 1B) display a prevalent fluorescent signal located in the nucleus (left panel), in agreement with the known targeting of Sam68 to this compartment, but a cytosolic and nuclear localization of Sam68 can also be observed in some cells (right panel). In Fig. 1C–E the expression of the C-terminus deleted forms, Sam68(1–355)-YFP, Sam68(1–335)-YFP and Sam68(1–295)-YFP, respectively, were exclusively restricted to cytosol as would be expected for Sam68 isoforms lacking the nuclear localization signal located along 420–443 aminoacids. In contrast, in Fig. 1F and G the expression of N-terminus deleted forms of Sam68, where NLS is present, Sam68(72–443) and Sam68(93–443), showed again the typical nuclear localization of Sam68 wild-type, (left panel), although in some cells a cytoplasmic and nuclear distribution was observed (right panel), as seen for full-length Sam68. All these constructs were also detected on a western blot of cell lysates (Fig. 1H), where the molecular weight and expression level of each construct can be evaluated using an anti-GFP antibody.

3.2. Study of interactions between insulin signaling effectors and Sam68 by BRET

The BRET methodology allows us to study the interaction between two partners, one fused to Renilla luciferase (Rluc) and the other partner fused to a yellow fluorescent protein (YFP). The luciferase transforms its substrate coelenterazine into a luminescent molecule that produces light at 480 nm. If the two partners interact (if the distance between the two partners is less than 100 Å), an energy transfer can occur between the Rluc and the YFP, resulting in the emission of a fluorescent signal by the YFP at 530 nm. This technique has been used to monitor ligand-induced conformational changes within the IR [42], as well as its interactions with other receptors or proteins [44,45,47,49], dimerization of G protein coupled receptors GPCR [52,53], and dimerization of other proteins [54,55].

The association of Sam68 to PI3K through the SH2 domains of the p85 regulatory subunit has previously been shown to link Sam68 to IR/IRS-1/p85PI3K complex in HTC-IR [24,25]. To determine whether these interactions could be detected by BRET, IR-Luc, IRS1(1–271)-YFP and p85α-YFP and Sam68 fused to either YFP or luciferase were used. In HEK293 expressing IR-Luc and Sam68-YFP or Sam68-Luc and p85α-YFP, no BRET signal could be detected (data not shown). These results indicate that if a direct interaction really takes place between Sam68 and IR or p85α, the relative orientation between these partners would not be favorable to energy transfer. Indeed, BRET signal not only depends on the distance between the luminescent and fluorescent proteins, but also on their relative orientation [56], and therefore, the absence of a detectable BRET signal does not necessarily means lack of interaction. In contrast, co-expression of Sam68-Luc and IRS1-YFP proteins in HEK-293 cells resulted in a robust BRET signal (around 100 mBU) that was measured during 15 min (Fig. 2A), suggesting a strong interaction between these proteins in basal conditions (open squares). Stimulation with insulin 100 nM of cells co-transfected with Sam68-Luc and IRS1-YFP (black solid squares) had no effect on the BRET signal, probably because HEK293 cells only express low endogen IR levels. The specificity of the signal was demonstrated by comparison with the low non-specific BRET signal obtained in cells transfected with Sam68-Luc and YFP (black circles), despite similar expression levels.

To further demonstrate the specificity of Sam68-Luc/IRS1-YFP interaction, we performed BRET donor saturation assays. In this kind of experiments, the donor concentration is kept constant while the acceptor concentration is increased. Thus, the BRET signal should rise with increasing acceptor concentrations until

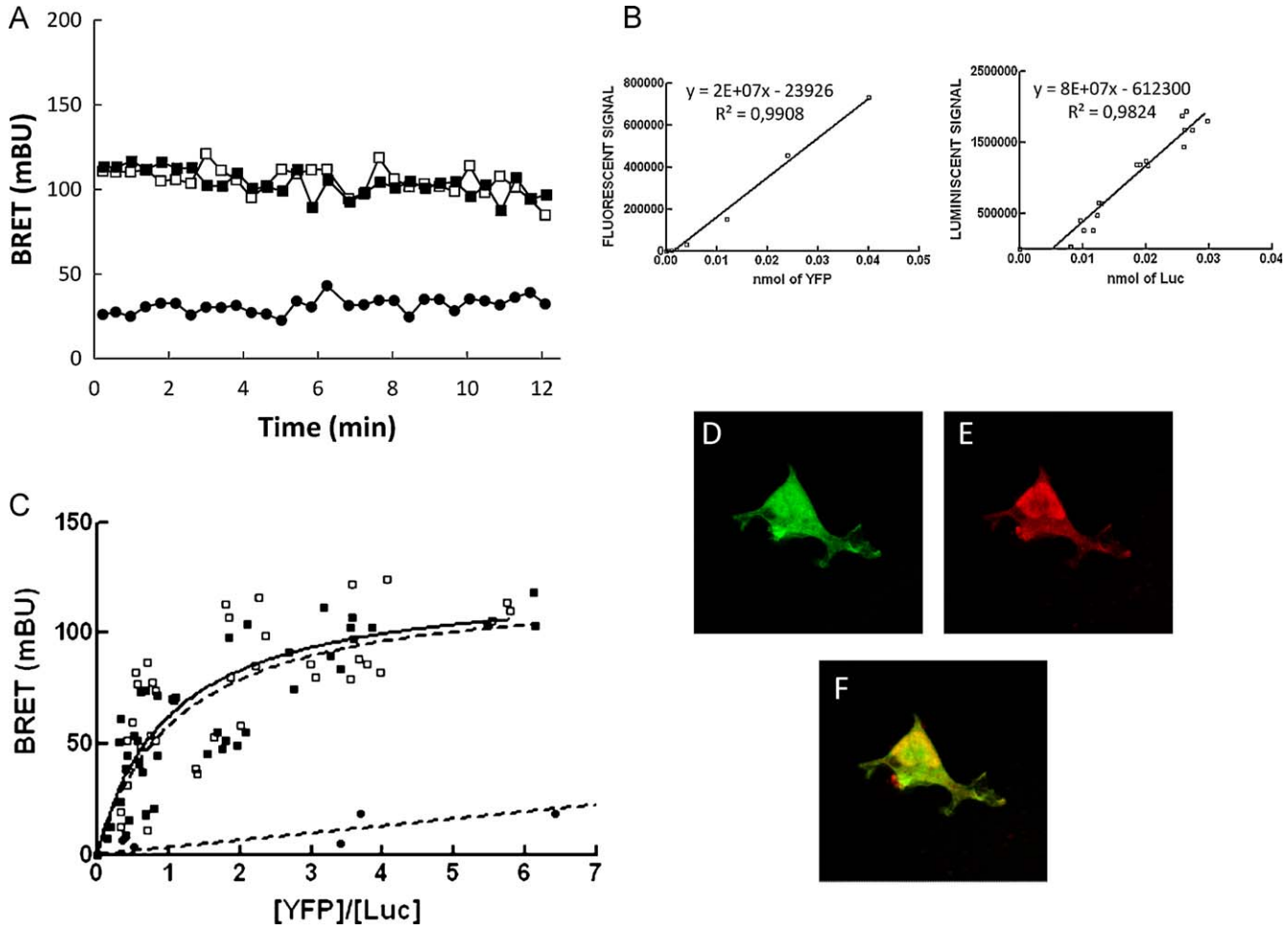

Fig. 2. Sam68-Luc/IRS1-YFP interaction can be measured by BRET. (A) HEK293 cells transfected with Sam68-Luc and either IRS1-YFP or YFP were pre-incubated 15 min with coelenterazine and then stimulated or not with 100 nM insulin. BRET measurements were started immediately after insulin stimulation. Data are representative of three experiments with a [YFP]/[Luc] ratio of 4. (B) Regression functions of YFP and luciferase signal. Known amounts of a commercial recombinant YFP protein were used to establish a standard curve permitting to convert fluorescent signals measured in BRET conditions assay into nmol of YFP molecules (left panel). For luciferase regression function, HEK293 cells were transfected with increasing amounts of cDNA encoding luciferase fused to YFP. Luminescent and fluorescent signals were measured in similar conditions as in BRET assays. The luminescent signal was plotted as a function of nmoles of YFP protein (obtained using the standard curve obtained previously to convert fluorescent signal into nmol of YFP molecules). Since each luciferase molecule was fused to one YFP molecule, luminescent signals could then be converted in nmol of luciferase molecules. Thus, a regression curve permitting to convert luminescent signal into nmol of luciferase molecules was obtained (right panel). (C) BRET saturation curve of IRS-1-YFP. HEK293 cells were transfected with a fixed amount of Sam68-luc cDNA (300 ng) and variable amounts of IRS1-YFP cDNA (50–2000 ng) and were stimulated (black solid squares) or not (open squares) with 100 nM of insulin. HEK293 also were transfected with Sam68-Luc and increasing amounts of EYFP-N1 cDNA (black solid circles) as negative control. The BRET ratio (expressed in mBU) is represented as a function of the [YFP]/[Luc] fusion protein ratio (quotient of nmoles of luciferase and nmoles of YFP obtained from regression curves of luciferase and YFP). Every saturation curve was constructed with at least 50 points from 4 independent experiments. (D-F) HEK293 cells were co-transfected with both IRS1-YFP and Sam68-Luc. By confocal microscopy, direct IRS1-YFP fluorescence signal is shown in panel D and indirect fluorescence corresponding to Sam68-Luc detected by immunocytochemistry is shown in panel E. In panel F, the two images were superimposed and the yellow color indicates co-localization of the two proteins.

reaching a plateau or maximum level where all donor molecules are engaged by an acceptor. At this point, the BRET signal denominated $BRET_{max}$, reflects the total number of donor–acceptor complexes and the distance between donor and acceptor molecules as well as their relative orientations, although, these two last factors are closely dependent on each construction [49,57–59]. The relative amount of acceptor to donor that gives 50% of the maximal energy transfer ($BRET_{50}$) reflects the relative affinity between donor- and acceptor-fusion proteins [44,49].

The BRET signal was measured in HEK293 cells transfected with a constant amount of Sam68-Luc cDNA and increasing amounts of IRS1-YFP or YFP. The BRET signal was plotted as a function of the fusion protein ratio [YFP]/[RLuc]. The fusion protein ratio was calculated as the (YFP nmoles)/(Luc nmoles) quotient. The fluorescent signal of the YFP was converted in nmoles of YFP proteins from a regression curve using fluorescence measurements of a recombinant YFP protein (Fig. 2B, left panel). The luciferase signal was converted in nmoles using a construction coding Luc and YFP proteins together. In this case, the expression of these two proteins is, by definition, equimolar, and allowed us to establish the regression curve for luminescent signal (Fig. 2B, right panel). Then, the BRET signal data expressed in mBU were fitted by using a non-linear regression equation assuming a single binding site (GraphPad Prism 5). As can be seen in Fig. 2C the BRET signal increases hyperbolically with crescent expression of acceptor construction (IRS-1-YFP), which implicates a specific interaction between Sam68-Luc and IRS-1-YFP when compared to the linear curve generated with non-saturatable "bystander" BRET obtained with YFP alone. $BRET_{50}$ calculated as the relative concentration of YFP (nM) over Luc (nM), was around 1 (Table 1), suggesting that the affinity between the partners is relatively high since equimolar amounts of the two partners resulted in half-saturation of the donor. Insulin stimulation of the cells had no effect, neither on $BRET_{max}$, nor on $BRET_{50}$ (Table 1).

Table 1
$BRET_{max}$ and $BRET_{50}$ parameters of Sam68-Luc/IRS1-YFP interaction.

	$BRET_{max}$	$BRET_{50}$
Sam68-Rluc + IRS1-YFP (Basal) (1)	123.7 ± 11.8	1.0 ± 0.2
Sam68-Rluc + IRS1-YFP (Ins 100 nM)	127.1 ± 11.5	1.1 ± 0.2

We next examined by confocal microscopy the location of Sam68-Luc/IRS1-YFP interaction. As shown in Fig. 2 (panels D–G), co-expression of IRS1-YFP and Sam68-Luc resulted in significant overlap of fluorescence signal in the cytosol as well as in the nucleus.

3.3. Mapping the region of Sam68 implicated in the interaction with IRS-1

IRS proteins contain a conserved pleckstrin homology (PH) domain at their amino termini, flanked by a phosphotyrosine binding (PTB) domain. Multiple Tyr and Ser/Thr phosphorylation motifs responsible for the propagation of IR signaling as well as its modulation are found in C-terminal to the PTB domain [36,37]. In this work, an IRS1-YFP construction has been used encoding only the conserved region of 271 amino acids (PH/PTB domain) fused to YFP protein (Fig. 1A). Indeed, previous studies have indicated that full length IRS1-fluorescent protein fusion is not properly expressed and forms aggregates into the cell [51]. The resulting IRS1 protein, containing only the PH and PTB domain, is capable of interacting with IR by its PTB domain [46,51].

To identify the Sam68 region implicated in the interaction with IRS1 we expressed proteins lacking one, two or three proline rich domains, in both N and C-terminals of Sam68 and we analyzed how these deletions modified the $BRET_{50}$ (see Fig. 1 for schematic diagram of truncated proteins). As shown in Fig. 3A, deletion of the C-terminal P5 proline rich domains, produced a rightward displacement of the saturation curve compared to wild-type interaction, resulting in a 2-fold increase in $BRET_{50}$ of Sam68(1–355)-Luc/IRS-1-YFP interaction over wild-type interaction (Table 2). The same result was obtained when the construct of Sam68 lacking P4 and P5 domains was used. Nonetheless, the deletion of three proline rich domains in C-terminus, P5, P4 and P3, restored a $BRET_{50}$ value similar to that of wild-type interaction. Such an increase in $BRET_{50}$ of Sam68(1–355)-Luc and Sam68(1–335)-Luc/IRS-1-YFP interactions indicates a diminished affinity between donor and acceptor, and suggests that the C-terminus region in Sam68 is important for its interaction with IRS1. On the other hand, $BRET_{50}$ of Sam68(71–443)-Luc/IRS1-YFP and Sam68(93–443)-Luc/IRS1-YFP interactions (Fig. 3B) were 2.5- and 1.8-fold higher than wild-type interaction. This decrease in affinity also gives a role for N-terminus region of Sam68.

Table 2
$BRET_{max}$ and $BRET_{50}$ of Sam68-Luc deleted isoforms/IRS1 interactions.

	$BRET_{max}$	$BRET_{50}$
Sam68(1–355)-Rluc + IRS1-YFP (2)	250.7 ± 26.1	2.0 ± 0.4
Sam68(1–335)-Rluc + IRS1-YFP (3)	280.2 ± 20.8	2.1 ± 0.3
Sam68(1–295)-Rluc + IRS1-YFP (4)	97.1 ± 13.0	1.1 ± 0.4
Sam68(71–443)-Rluc + IRS1-YFP (5)	115.3 ± 17.15	2.5 ± 0.9
Sam68(93–443)-Rluc + IRS1-YFP (6)	121.7 ± 19.2	1.8 ± 0.6

The interaction of IRS1(1–271)-YFP with the different variants of Sam68 tagged with Luc was also demonstrated by immunoprecipitation with an anti-GFP antibody (Fig. 4). HEK cells were co-transfected with 300 ng cDNA of IRS1-YFP and 300 ng cDNA of either empty vector or for full-length or truncated Sam68-Luc. When different constructs are overexpressed in a cell, the protein expression level is not necessarily the same. This was the case with the different deleted mutants of Sam68-Luc. As can be seen in Fig. 4A, the transfection of HEK293 cells with full-length Sam68-Luc and the five Sam68-Luc truncated mutants results in different protein expression levels, as detected in lysates by western blotting with an anti-luciferase antibody. Immunoprecipitation of IRS1 was performed using an anti-GFP antibody, and the amount of Sam68 co-immunoprecipitated with IRS1 was evaluated using an anti-luciferase antibody (Fig. 4B). The quantification of luciferase signal in western blot showed important differences in the amount of luciferase-tagged proteins bound to IRS1-YFP. However, when the luciferase signal in the immunoprecipitate was corrected by the amount of luciferase present in the cell lysate (Fig. 4C), it appeared that Sam68-Luc, Sam68(1–295)-Luc and Sam68(93–443)-Luc were very similar in their capacity to bind to IRS1-YFP, whereas Sam68(1–355)-Luc, Sam68(1–335)-Luc and Sam68(71–443)-Luc bound IRS1-YFP less efficiently.

3.4. Effect of IR overexpression on Sam68-Luc/IRS1-YFP interaction

The expression of endogenous IR in HEK293 cells is very low [44]; hence we were not able to see any insulin effect on Sam68-Luc/IRS1-YFP interaction (Fig. 1). To determine whether this

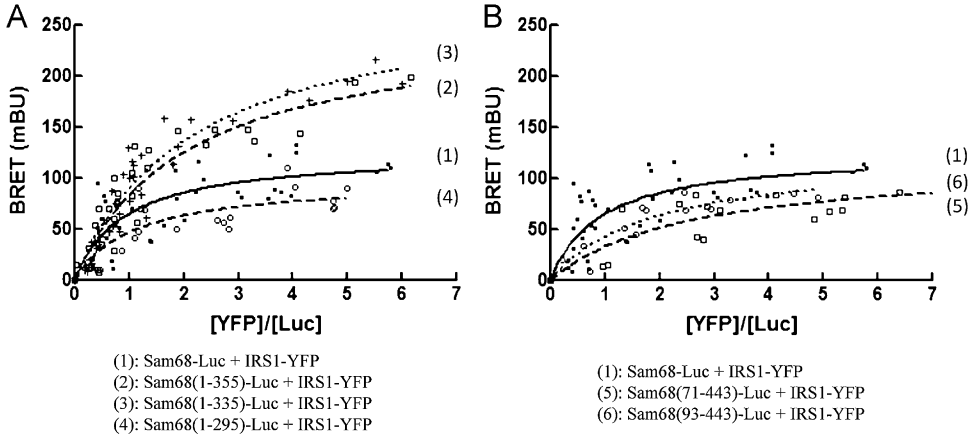

Fig. 3. Mapping the domains of Sam68 implicated in the interaction with IRS1. BRET saturation experiments were performed using HEK293 cells co-transfected with fixed amounts of wild-type or truncated mutants of Sam68-Luc cDNAs and crescent amounts of IRS1-YFP cDNA. (A) Curve 1: Sam68-Luc/IRS1-YFP interaction (continuous line, black squares); curve 2: Sam68(1–355)-Luc/IRS1-YFP interaction (discontinuous line, open squares); curve 3: Sam68(1–335)/IRS1-YFP (punctuated line, crosses); curve 4: Sam68(1–295)-Luc/IRS1-YFP (discontinuous line, open circles). (B) Curve 1: Sam68-Luc/IRS1-YFP interaction (continuous line, black squares); curve 5: Sam68(71–443)-Luc/IRS1-YFP interaction (discontinuous line with open circles); curve 6: Sam68(93–443)-Luc/IRS1-YFP interaction (punctuated line, open squares). Each curve was constructed with 25–40 points from 3 to 4 independent experiments.

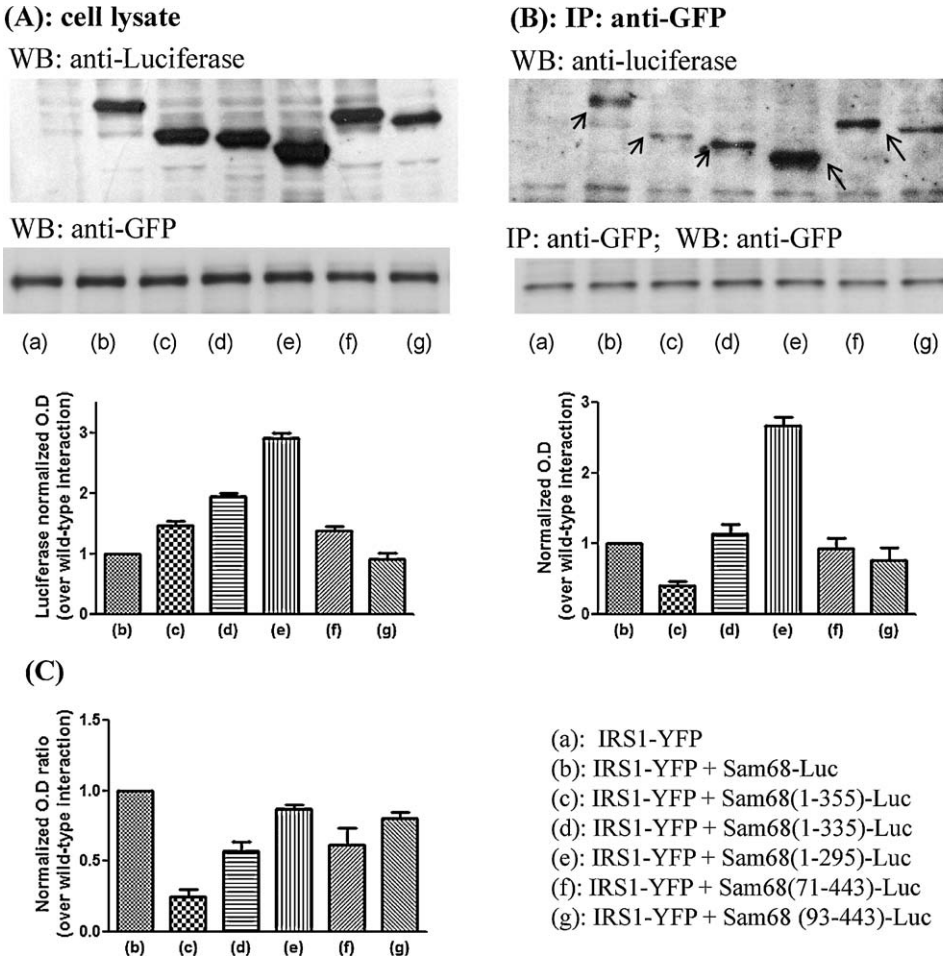

Fig. 4. Detection of the interaction between IRS1 and wild-type or deletion mutants of Sam68 by immunoprecipitation. HEK293 seeded in 10 cm dishes were transfected with IRS1-YFP and the different deleted forms of Sam68-Luc. Two days after transfection, cells were lysed and immunoprecipitated with anti-GFP antibody. The proteins in total cell lysates as well as immunoprecipitated proteins were separated on 7% SDS-polyacrylamide gels, transferred to nitrocellulose, and immunoblotted with anti-luciferase and anti-GFP antibodies. (A) Western blotting of a whole lysate of transfected cells with anti-luciferase or anti-GFP antibodies (upper panel), and optical density (O.D., middle panel) of the luciferase signal. (B) Western blot (upper panel) with anti-luciferase and anti-GFP antibodies of the proteins immunoprecipitated with anti-GFP antibody. Immunoprecipitated Sam68-Luc, Sam68(1–355)-Luc, Sam68(1–335)-Luc, Sam68(1–295) and Sam68(71–443) are indicated by arrows. The middle panel shows optical densities (O.D.) of the immunoprecipitated luciferase signals. (C) Relative amounts of Sam68-Luc mutants co-immunoprecipitated with IRS-YFP after normalization by the amount of Sam-68-Luc mutant present in each cell extract ([O.D. from IP/O.D. from lysates] ratio). Western blots are representative of three experiments.

interaction can be modulated by insulin, HEK293 cells were co-transfected with Sam68-Luc, IRS1-YFP and IR cDNAs, maintaining Sam68-Luc and IR expression constant while increasing the IRS1-YFP (Fig. 5A). BRET saturation curves indicate that in basal condition, $BRET_{50}$ was 0.7. When insulin was present, the $BRET_{50}$ decreased to 0.3 (Table 3). This increase in affinity suggests that insulin promotes recruitment of IRS1 to Sam68 [49,60].

We also wanted to determine if different levels of IR overexpression might affect Sam68-Luc/IRS1-YFP saturation curves (Fig. 5B). To this aim, we transfected HEK293 cells with increasing amounts of IR cDNA (300, 400 and 600 ng). The expression level of the IR was controlled by western blotting (Fig. 5C). The effect of IR overexpression on $BRET_{50}$ is shown in Table 3. Increasing the amounts of IR expression level resulted in a decrease in $BRET_{50}$ of Sam68-Luc/IRS1-YFP interaction, although transfection of 400 and 600 ng of cDNA gave the same $BRET_{50}$.

4. Discussion

4.1. The interaction between Sam68 and IRS1

Previous works by our group have proposed a role for Sam68 in IR signaling pathway [23]. In HTC overexpressing IR, insulin has been shown to have a dose-dependent effect on Sam68 tyrosine phosphorylation. In CHO cells overexpressing IR and in a more physiological system such as isolated rat adipocytes, a similar effect of insulin on Sam68 tyrosine phosphorylation was found [22,25]. After its phosphorylation in response to insulin, Sam68 is recruited from nucleus to different insulin signaling complexes located in the cytosol such as IRS1/PI3K [25], Ras-GAP [6,16] or Grb2-SOS [26]. Moreover, in an important insulin target cell as rat adipocytes, localization of Sam68 in basal conditions is preeminently cytosolic [22]. In this paper, we demonstrate for the first time that Sam68 directly interacts with IRS1. Co-localization of Sam68 and IRS1 was observed by confocal microscopy both in the nucleus and the cytosol (Fig. 2) suggesting that interaction between these partners could take place in both compartments. The fact that Sam68/IRS1 interaction can be detected with an IRS1 construction which contains only the first 271 N-terminal residues (i.e. comprising the PH and PTB domains but lacking most tyrosine phosphorylation sites) suggests that Sam68/IRS1 interaction is independent of tyrosine phosphorylation of IRS1 by IR.

4.2. Domains of Sam68 implicated in the interaction with IRS1

Our BRET experiments indicate that the interaction between Sam68 and IRS1 seems to implicate both N and C termini end of Sam68. The increase in $BRET_{50}$ of Sam68(1–355)-Luc/IRS-1-YFP

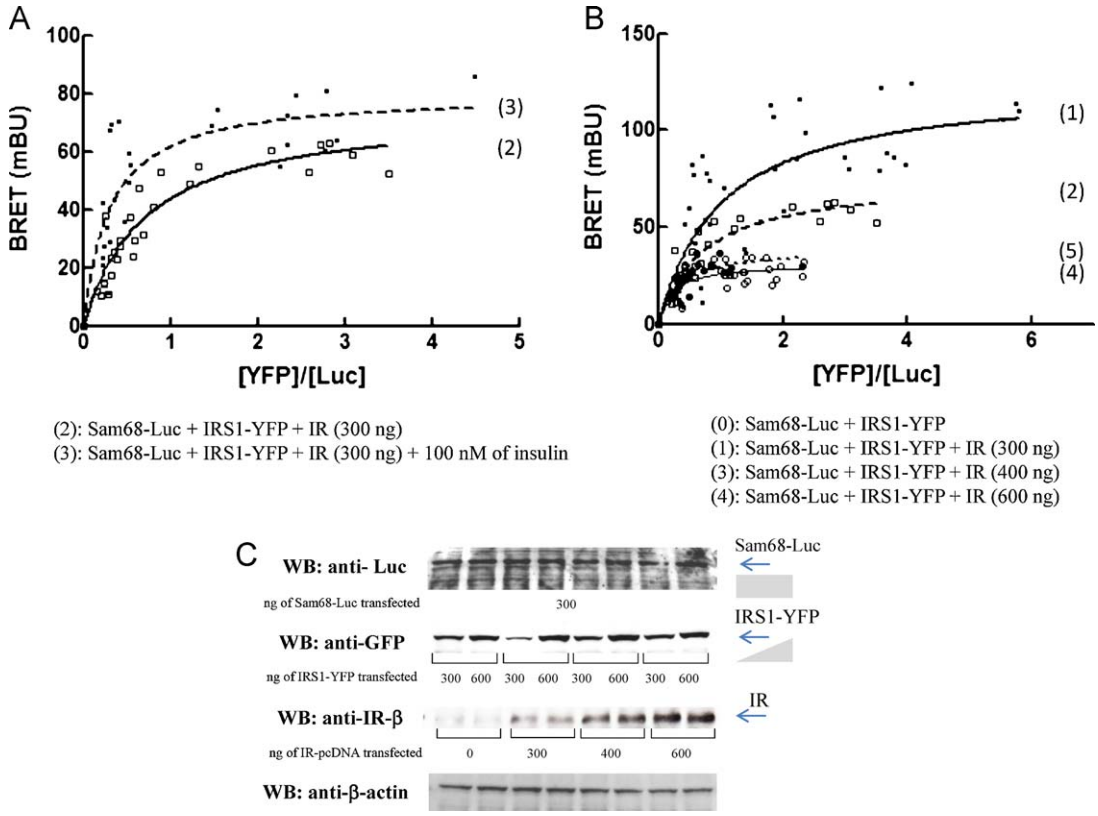

Fig. 5. Effect of IR overexpression and insulin stimulation on Sam68-Luc/IRS1-YFP interaction. (A) Basal and insulin stimulated BRET saturation curves. The cells were co-transfected with fixed amounts of Sam68-Luc and IR-pcDNA3 (300 ng of both cDNAs) and crescent amounts of IRS1-YFP cDNA in absence (continuous curve 2, open squares) or presence of 100 nM of insulin (discontinuous curve 3, black squares). (B) Comparison of saturation curves of Sam68-Luc/IRS1-YFP interaction when HEK293 cells are co-transfected with crescent amounts of IR-pCDNA3.1. Continuous curve 1 (black squares) is the saturation curve obtained for Sam68-Luc/IRS1-YFP interaction in absence of transfected IR; discontinuous curve 2 (open squares) is the saturation curve for the same interaction when the cells were co-transfected with 300 ng of IR-pcDNA; continuous curve 4 (open circles) is the saturation curve obtained when the cells were co-transfected with 400 ng of IR-pcDNA3; punctuated curve 5 (black circles) is the saturation curve obtained when the cells were co-transfected with 600 ng of IR-pcDNA3. (C) Control of IR amount expressed in HEK293 cells co-expressing Sam68-Luc and IRS1-YFP by immunoblotting. A fraction of the cells used in a representative BRET experiment shown in (B) were lysed. Proteins were denatured, electrophoretically resolved in 7% SDS-PAGE and transferred to a nitrocellulose membrane. Sam68-Luc, IRS1-YFP and IR and β-actin proteins were immunodetected by using anti-luciferase, anti-GFP, anti-IRβ and anti-β-actin antibodies. Each curve include between 25 and 43 experimental points.

and Sam68(1–335)-Luc/IRS-1-YFP interactions in comparison to that of wild-type Sam68, indicates a lower affinity of these isoforms for IRS1, suggesting that the C-terminus region of Sam68 comprising of at least the aminoacids 355 to 443 is implicated in the interaction with IRS1. Intriguingly, the deletion of P3 together with P4 and P5 proline rich domains restores the binding affinity of Sam68 to IRS1. This finding indicates that P3 domain is implicated in some functions of Sam68 that depending on signal transduction and cellular processes, might modulate the interaction with IRS1. The absence of aminoacids 1–70 (containing, proline rich domains P0 and P1 in N terminus) also decreased the affinity of Sam68(71–443)-Luc/IRS1-YFP suggesting a role to these domains for Sam68/IRS1 interaction.

The GSG domain of Sam68 is common to other members of STAR proteins, this domain is a hnRNPKhomology (KH) domain flanked by two domains in N- and C-terminal, known as Qua1 (amino acids from 95 to 135 in Sam68) and Qua2 (amino acids from 256 to 280 in Sam68), respectively [61,62]. The capacity to oligomerize is attributed to Qua1 domain, whereas Qua2 is thought to be essential for sequence specific RNA recognition [63]. In our BRET assays, Qua2 and Qua1 were present in all constructs used. This suggests that IRS1 may interact with dimeric or oligomeric forms of Sam68.

4.3. Sam68/IRS1 interaction and IR signaling

The other question we want to address is the possible role that Sam68/IRS1 interaction could have in IR signaling. As HEK293 did not express a significant level of IR, we overexpressed IR in cells co-expressing both Sam68-Luc and IRS1- YFP partners of BRET. The presence of IR produces an increase in affinity of Sam68/IRS1 interaction meaning that a recruitment of IRS1 to Sam68 is produced. Crescent overexpression of IR also reveals a dependent increase in affinity with a reduction in $BRET_{max}$ of Sam68/IRS1 interaction. This decrease in $BRET_{max}$ may be a consequence of the presence of IR, which by interacting with IRS1 or Sam68, may change the efficiency of energy transfer between Sam68-Luc and

Table 3
$BRET_{max}$ and $BRET_{50}$ of Sam68-Luc/IRS1-YFP interaction with different level of IR expression.

	$BRET_{max}$	$BRET_{50}$
Sam68-Rluc/IRS1-YFP/IR (300 ng of cDNA) Basal (2)	74.3 ± 5.1	0.7 ± 0.1
Sam68-Rluc/IRS1-YFP/IR (300 ng of cDNA) Ins 100 nM (3)	78.6 ± 6.2	0.3 ± 0.06
Sam68-Rluc/IRS1-YFP/IR (400 ng of cDNA) (4)	31.0 ± 2.5	0.2 ± 0.09
Sam68-Rluc/IRS1-YFP/IR (600 ng of cDNA) (5)	38.4 ± 4.4	0.3 ± 0.1

IRS1-YFP. Taken together, these results suggest that Sam68, interacts with IRS1 in basal conditions and that insulin stimulation increases the affinity of Sam68/IRS1 interaction when IR is present.

4.4. Possible implications of Sam68/IRS1 interaction

The importance in describing Sam68/IRS1 interaction stems from various data that implicates both proteins in oncogenic transformation and cancer progression as breast cancer or prostate cancer [38,64–68]. Curiously Sam68 and IRS1 have been implicated in the regulation of transcriptional activity of estrogen and androgen receptor in nucleus [39,67–69].

Other proteins without SH2 domains have been reported to bind IRS1. Thus, it has been shown that phosphorylated IRS1 and IRS2 are capable of binding to and regulating proteins devoided of SH2 domains such as Bcl-2, 14-3-3 adaptor proteins or the focal adhesion kinase $pp124^{FAK}$ [70–74]. On the other hand, the function of PH domains is the targeting of proteins to membranes by binding phosphoinositides [75]. Several proteins containing PH domains have to bind certain proteins known as, PH domain-protein ligands, to ensure effective membrane association and subsequent activation of signaling pathways. For example, the association of PH domain of β-adrenergic receptor kinase (βARK) to Gβγ subunits of heterotrimeric G-proteins or the association of PH domains of pleckstrin and BTK to filamentous actin seem to be implicated in directing the localization of these PH domains containing proteins to the proximity of plasma membrane [76,77].

4.5. Conclusion

Our work indicate that Sam68 interacts with IRS1 in basal conditions and insulin stimulation as well as the overexpression of IR increase the affinity of this interaction in living cells. In this way, Sam68 could have a function at the first steps of IR signaling, by allowing or favoring the recruitment of IRS1 to IR proximity.

Acknowledgments

We thank to Ribas Salgueiro JL and Fernández Estéfene A from Microscopy Service of Centro de Investigación, Tecnología e Innovación de la Universidad de Sevilla (CITIUS) and to Fernández-Santos JM (Department of Normal and Pathological Cytology and Histology, School of Medicine, Seville) for the excellent help and assistance with the confocal microscopy. We also thank to Najib S (Institut de Médecine Moléculaire de Rangueil, Toulouse) for her invaluable work revising manuscript and to Santos-Alvarez J for discussion of results and correcting English language.

This work was supported by a research grant associated to a Miguel Servet contract CP05/00273 from the Instituto de Salud Carlos III (Spanish Ministry of Health), by a grant from Spanish Ministry of Science and Innovation SAF2008-03433 and by a grant of Consejería de Salud de la Junta de Andalucía PI-0055.

Quintana-Portillo R and Canfrán-Duque A were recipients of research fellowships from Sanitary Association of Virgen Macarena Hospital.

References

[1] Dreyfuss G, Matunis MJ, Pinol-Roma S, Burd CG. hnRNP proteins and the biogenesis of mRNA. Annu Rev Biochem 1993;62:289–321.
[2] Fumagalli S, Totty NF, Hsuan JJ, Courtneidge SA. A target for Src in mitosis. Nature 1994;368:871–4.
[3] Taylor SJ, Shalloway D. An RNA-binding protein associated with Src through its SH2 and SH3 domains in mitosis. Nature 1994;368:867–71.
[4] Espejo A, Cote J, Bednarek A, Richard S, Bedford MT. A protein-domain microarray identifies novel protein–protein interactions. Biochem J 2002; 367:697–702.
[5] Bedford MT, Reed R, Leder P. WW domain-mediated interactions reveal a spliceosome-associated protein that binds a third class of proline-rich motif: the proline glycine and methionine-rich motif. Proc Natl Acad Sci USA 1998;95:10602–7.
[6] Taylor SJ, Anafi M, Pawson T, Shalloway D. Functional interaction between c-Src and its mitotic target, Sam 68. J Biol Chem 1995;270:10120–4.
[7] Maa MC, Leu TH, Trandel BJ, Chang JH, Parsons SJ. A protein that is highly related to GTPase-activating protein-associated p62 complexes with phospholipase C gamma. Mol Cell Biol 1994;14:5466–73.
[8] Richard S, Yu D, Blumer KJ, Hausladen D, Olszowy MW, Connelly PA, et al. Association of p62, a multifunctional SH2- and SH3-domain-binding protein, with src family tyrosine kinases, Grb2, and phospholipase C gamma-1. Mol Cell Biol 1995;15:186–97.
[9] Trub T, Frantz JD, Miyazaki M, Band H, Shoelson SE. The role of a lymphoid-restricted, Grb2-like SH3-SH2-SH3 protein in T cell receptor signaling. J Biol Chem 1997;272:894–902.
[10] Lawe DC, Hahn C, Wong AJ. The Nck SH2/SH3 adaptor protein is present in the nucleus and associates with the nuclear protein SAM68. Oncogene 1997;14:223–31.
[11] Sette C. Post-translational regulation of star proteins and effects on their biological functions. Adv Exp Med Biol 2010;693:54–66.
[12] Vogel LB, Fujita DJ. p70 phosphorylation and binding to p56lck is an early event in interleukin-2-induced onset of cell cycle progression in T-lymphocytes. J Biol Chem 1995;270:2506–11.
[13] Derry JJ, Richard S, Valderrama CH, Ye X, Vasioukhin V, Cochrane AW, et al. Sik (BRK) phosphorylates Sam68 in the nucleus and negatively regulates its RNA binding ability. Mol Cell Biol 2000;20:6114–26.
[14] Andreotti AH, Bunnell SC, Feng S, Berg LJ, Schreiber SL. Regulatory intramolecular association in a tyrosine kinase of the Tec family. Nature 1997;385: 93–7.
[15] Bunnell SC, Henry PA, Kolluri R, Kirchhausen T, Rickles RJ, Berg LJ. Identification of Itk/Tsk Src homology 3 domain ligands. J Biol Chem 1996;271:25646–5.
[16] Guitard E, Barlat I, Maurier F, Schweighoffer F, Tocque B. Sam68 is a Ras-GAP-associated protein in mitosis. Biochem Biophys Res Commun 1998;245:562–6.
[17] Chen T, Boisvert FM, Bazett-Jones DP, Richard S. A role for the GSG domain in localizing Sam68 to novel nuclear structures in cancer cell lines. Mol Biol Cell 1999;10:3015–33.
[18] Ishidate T, Yoshihara S, Kawasaki Y, Roy BC, Toyoshima K, Akiyama T. Identification of a novel nuclear localization signal in Sam68. FEBS Lett 1997;409:237–41.
[19] Cote J, Boisvert FM, Boulanger MC, Bedford MT, Richard S. Sam68 RNA binding protein is an in vivo substrate for protein arginine N-methyltransferase 1. Mol Biol Cell 2003;14:274–87.
[20] Reddy TR, Xu W, Mau JK, Goodwin CD, Suhasini M, Tang H, et al. Inhibition of HIV replication by dominant negative mutants of Sam68, a functional homolog of HIV-1 Rev. Nat Med 1999;5:635–42.
[21] Bielli P, Busa R, Paronetto MP, Sette C. The RNA binding protein Sam68 is a multifunctional player in human cancer. Endocr Relat Cancer 2011;18(4):R91–102.
[22] Sanchez-Margalet V, Gonzalez-Yanes C, Najib S, Fernandez-Santos JM, Martin-Lacave I. The expression of Sam68, a protein involved in insulin signal transduction, is enhanced by insulin stimulation. Cell Mol Life Sci 2003;60: 751–8.
[23] Najib S, Martin-Romero C, Gonzalez-Yanes C, Sanchez-Margalet V. Role of Sam68 as an adaptor protein in signal transduction. Cell Mol Life Sci 2005;62:36–43.
[24] Sung CK, Sanchez-Margalet V, Goldfine ID. Role of p85 subunit of phosphatidylinositol-3-kinase as an adaptor molecule linking the insulin receptor, p62, and GTPase-activating protein. J Biol Chem 1994;269:12503–7.
[25] Sanchez-Margalet V, Najib S. p68 Sam is a substrate of the insulin receptor and associates with the SH2 domains of p85 PI3K. FEBS Lett 1999;455:307–10.
[26] Najib S, Sanchez-Margalet V. Sam68 associates with the SH3 domains of Grb2 recruiting GAP to the Grb2–SOS complex in insulin receptor signaling. J Cell Biochem 2002;86:99–106.
[27] Sanchez-Margalet V, Najib S. Sam68 is a docking protein linking GAP and PI3K in insulin receptor signaling. Mol Cell Endocrinol 2001;183:113–21.
[28] Sun XJ, Wang LM, Zhang Y, Yenush L, Myers Jr MG, Glasheen E, et al. Role of IRS-2 in insulin and cytokine signalling. Nature 1995;377:173–7.
[29] Smith-Hall J, Pons S, Patti ME, Burks DJ, Yenush L, Sun XJ, et al. The 60 kDa insulin receptor substrate functions like an IRS protein (pp60IRS3) in adipose cells. Biochemistry 1997;36:8304–10.
[30] Lavan BE, Lane WS, Lienhard GE. The 60-kDa phosphotyrosine protein in insulin-treated adipocytes is a new member of the insulin receptor substrate family. J Biol Chem 1997;272:11439–43.
[31] Lavan BE, Fantin VR, Chang ET, Lane WS, Keller SR, Lienhard GE. A novel 160-kDa phosphotyrosine protein in insulin-treated embryonic kidney cells is a new member of the insulin receptor substrate family. J Biol Chem 1997;272:21403–7.
[32] Cai D, Dhe-Paganon S, Melendez PA, Lee J, Shoelson SE. Two new substrates in insulin signaling, IRS5/DOK4 and IRS6/DOK5. J Biol Chem 2003;278: 25323–30.
[33] Sawka-Verhelle D, Tartare-Deckert S, White MF, Van OE. Insulin receptor substrate-2 binds to the insulin receptor through its phosphotyrosine-binding domain and through a newly identified domain comprising amino acids 591–786. J Biol Chem 1996;271:5980–3.

[34] Voliovitch H, Schindler DG, Hadari YR, Taylor SI, Accili D, Zick Y. Tyrosine phosphorylation of insulin receptor substrate-1 in vivo depends upon the presence of its pleckstrin homology region. J Biol Chem 1995;270:18083–7.
[35] Myers Jr MG, White MF. The new elements of insulin signaling. Insulin receptor substrate-1 and proteins with SH2 domains. Diabetes 1993;42:643–50.
[36] Taniguchi CM, Emanuelli B, Kahn CR. Critical nodes in signalling pathways: insights into insulin action. Nat Rev Mol Cell Biol 2006;7:85–96.
[37] Saltiel AR, Pessin JE. Insulin signaling pathways in time and space. Trends Cell Biol 2002;12:65–71.
[38] Dearth RK, Cui X, Kim HJ, Hadsell DL, Lee AV. Oncogenic transformation by the signaling adaptor proteins insulin receptor substrate (IRS)-1 and IRS-2. Cell Cycle 2007;6:705–13.
[39] Morelli C, Garofalo C, Sisci D, del RS, Cascio S, Tu X, et al. Nuclear insulin receptor substrate 1 interacts with estrogen receptor alpha at ERE promoters. Oncogene 2004;23:7517–26.
[40] Sisci D, Morelli C, Cascio S, Lanzino M, Garofalo C, Reiss K, et al. The estrogen receptor alpha:insulin receptor substrate 1 complex in breast cancer: structure–function relationships. Ann Oncol 2007;18(Suppl. 6):vi81–5.
[41] Chen J, Wu A, Sun H, Drakas R, Garofalo C, Cascio S, et al. Functional significance of type 1 insulin-like growth factor-mediated nuclear translocation of the insulin receptor substrate-1 and beta-catenin. J Biol Chem 2005;280:29912–20.
[42] Issad T, Boute N, Pernet K. A homogenous assay to monitor the activity of the insulin receptor using bioluminescence resonance energy transfer. Biochem Pharmacol 2002;64:813–7.
[43] Issad T, Blanquart C, Gonzalez-Yanes C. The use of bioluminescence resonance energy transfer for the study of therapeutic targets: application to tyrosine kinase receptors. Expert Opin Ther Targets 2007;11:541–56.
[44] Boute N, Pernet K, Issad T. Monitoring the activation state of the insulin receptor using bioluminescence resonance energy transfer. Mol Pharmacol 2001;60:640–5.
[45] Blanquart C, Gonzalez-Yanes C, Issad T. Monitoring the activation state of insulin/insulin-like growth factor-1 hybrid receptors using bioluminescence resonance energy transfer. Mol Pharmacol 2006;70:1802–11.
[46] Versteyhe S, Blanquart C, Hampe C, Mahmood S, Christeff N, De MP, et al. Insulin receptor substrates-5 and -6 are poor substrates for the insulin receptor. Mol Med Rep 2010;3:189–93.
[47] Boute N, Boubekeur S, Lacasa D, Issad T. Dynamics of the interaction between the insulin receptor and protein tyrosine-phosphatase 1B in living cells. EMBO Rep 2003;4:313–9.
[48] Laemmli UK. Cleavage of structural proteins during the assembly of the head of bacteriophage T4. Nature 1970;227:680–5.
[49] Nouaille S, Blanquart C, Zilberfarb V, Boute N, Perdereau D, Burnol AF, et al. Interaction between the insulin receptor and Grb14: a dynamic study in living cells using BRET. Biochem Pharmacol 2006;72:1355–66.
[50] Lukong KE, Larocque D, Tyner AL, Richard S. Tyrosine phosphorylation of sam68 by breast tumor kinase regulates intranuclear localization and cell cycle progression. J Biol Chem 2005;280:38639–47.
[51] Jacobs AR, LeRoith D, Taylor SI. Insulin receptor substrate-1 pleckstrin homology and phosphotyrosine-binding domains are both involved in plasma membrane targeting. J Biol Chem 2001;276:40795–802.
[52] Ayoub MA, Couturier C, Lucas-Meunier E, Angers S, Fossier P, Bouvier M, et al. Monitoring of ligand-independent dimerization and ligand-induced conformational changes of melatonin receptors in living cells by bioluminescence resonance energy transfer. J Biol Chem 2002;277:21522–8.
[53] Angers S, Salahpour A, Joly E, Hilairet S, Chelsky D, Dennis M, et al. Detection of beta 2-adrenergic receptor dimerization in living cells using bioluminescence resonance energy transfer (BRET). Proc Natl Acad Sci USA 2000;97:3684–9.
[54] Poulsen H, Jorgensen R, Heding A, Nielsen FC, Bonven B, Egebjerg J. Dimerization of ADAR2 is mediated by the double-stranded RNA binding domain. RNA 2006;12:1350–60.
[55] Germain-Desprez D, Bazinet M, Bouvier M, Aubry M. Oligomerization of transcriptional intermediary factor 1 regulators and interaction with ZNF74 nuclear matrix protein revealed by bioluminescence resonance energy transfer in living cells. J Biol Chem 2003;278:22367–73.
[56] Boute N, Jockers R, Issad T. The use of resonance energy transfer in high-throughput screening: BRET versus FRET. Trends Pharmacol Sci 2002;23:351–4.
[57] Bouvier M, Heveker N, Jockers R, Marullo S, Milligan G. BRET analysis of GPCR oligomerization: newer does not mean better. Nat Methods 2007;4:3–4.
[58] Mercier JF, Salahpour A, Angers S, Breit A, Bouvier M. Quantitative assessment of beta 1- and beta 2-adrenergic receptor homo- and heterodimerization by bioluminescence resonance energy transfer. J Biol Chem 2002;277:44925–31.
[59] Guan R, Feng X, Wu X, Zhang M, Zhang X, Hebert TE, et al. Bioluminescence resonance energy transfer studies reveal constitutive dimerization of the human lutropin receptor and a lack of correlation between receptor activation and the propensity for dimerization. J Biol Chem 2009;284:7483–94.
[60] Lacasa D, Boute N, Issad T. Interaction of the insulin receptor with the receptor-like protein tyrosine phosphatases PTPalpha and PTPepsilon in living cells. Mol Pharmacol 2005;67:1206–13.
[61] Lukong KE, Richard S. Sam68, the KH domain-containing superSTAR. Biochim Biophys Acta 2003;1653:73–86.
[62] Vernet C, Artzt K. STAR, a gene family involved in signal transduction and activation of RNA. Trends Genet 1997;13:479–84.
[63] Liu Z, Luyten I, Bottomley MJ, Messias AC, Houngninou-Molango S, Sprangers R, et al. Structural basis for recognition of the intron branch site RNA by splicing factor 1. Science 2001;294:1098–102.
[64] Chan BT, Lee AV. Insulin receptor substrates (IRSs) and breast tumorigenesis. J Mammary Gland Biol Neoplasia 2008;13:415–22.
[65] Elliott DJ, Rajan P. The role of the RNA-binding protein Sam68 in mammary tumourigenesis. J Pathol 2010;222:223–6.
[66] Song L, Wang L, Li Y, Xiong H, Wu J, Li J, et al. Sam68 up-regulation correlates with, and its down-regulation inhibits, proliferation and tumourigenicity of breast cancer cells. J Pathol 2010;222:227–37.
[67] Richard S, Vogel G, Huot ME, Guo T, Muller WJ, Lukong KE. Sam68 haploinsufficiency delays onset of mammary tumorigenesis and metastasis. Oncogene 2008; 17;27(4):548–56.
[68] Busa R, Paronetto MP, Farini D, Pierantozzi E, Botti F, Angelini DF, et al. The RNA-binding protein Sam68 contributes to proliferation and survival of human prostate cancer cells. Oncogene 2007;26:4372–82.
[69] Lanzino M, Garofalo C, Morelli C, Le PM, Casaburi I, McPhaul MJ, et al. Insulin receptor substrate 1 modulates the transcriptional activity and the stability of androgen receptor in breast cancer cells. Breast Cancer Res Treat 2009;115:297–306.
[70] Ueno H, Kondo E, Yamamoto-Honda R, Tobe K, Nakamoto T, Sasaki K, et al. Association of insulin receptor substrate proteins with Bcl-2 and their effects on its phosphorylation and antiapoptotic function. Mol Biol Cell 2000;11:735–46.
[71] Ogihara T, Isobe T, Ichimura T, Taoka M, Funaki M, Sakoda H, et al. 14-3-3 protein binds to insulin receptor substrate-1, one of the binding sites of which is in the phosphotyrosine binding domain. J Biol Chem 1997;272:25267–74.
[72] Kosaki A, Yamada K, Suga J, Otaka A, Kuzuya H. 14-3-3beta protein associates with insulin receptor substrate 1 and decreases insulin-stimulated phosphatidylinositol 3′-kinase activity in 3T3L1 adipocytes. J Biol Chem 1998;273:940–4.
[73] Lebrun P, Mothe-Satney I, Delahaye L, Van OE, Baron V. Insulin receptor substrate-1 as a signaling molecule for focal adhesion kinase pp125(FAK) and pp60(src). J Biol Chem 1998;273:32244–53.
[74] Lebrun P, Baron V, Hauck CR, Schlaepfer DD, Van OE. Cell adhesion and focal adhesion kinase regulate insulin receptor substrate-1 expression. J Biol Chem 2000;275:38371–7.
[75] Lemmon MA, Ferguson KM. Signal-dependent membrane targeting by pleckstrin homology (PH) domains. Biochem J 2000;350(Pt 1):1–18.
[76] Pitcher JA, Touhara K, Payne ES, Lefkowitz RJ. Pleckstrin homology domain-mediated membrane association and activation of the beta-adrenergic receptor kinase requires coordinate interaction with G beta gamma subunits and lipid. J Biol Chem 1995;270:11707–10.
[77] Ma AD, Abrams CS. Pleckstrin induces cytoskeletal reorganization via a Rac-dependent pathway. J Biol Chem 1999;274:28730–5.